

Electronic Supplementary Information

Self-standing hollow Ni-doped Mo₂C nano tube arrays induced by the Kirkendall effect for efficient hydrogen evolution reaction in acidic and alkaline solutions

Chen Li, Beirong Ye, Renhong Chen, Yongqi Li, Xin Liu, Tongwei Wu, Hongxian Liu,* Xinhui Xia, * Yongqi Zhang*

Prof. Y. Q. Zhang, Dr. T. Wu, C. Li, B. R. Ye, Y. Q. Li,

Institute of Fundamental and Frontier Sciences, University of Electronic Science and Technology of China, Chengdu 611371, China

Email: yqzhang@uestc.edu.cn

R. H. Chen,

School of Electrical Engineering, University of South China, Hengyang 421001, China

Prof. X. Liu,

State Key Laboratory of New Textile Materials & Advanced Processing Technology

Wuhan Textile University Wuhan 430073, China

Hongxian Liu, liu_hongxian@163.com

School of Physics and Electronic Science, Zunyi Normal University, Zunyi 563000,

Guizhou, China

Prof. X. H. Xia,

School of Materials Science & Engineering, Zhejiang University of Technology,

Hangzhou 310014, China

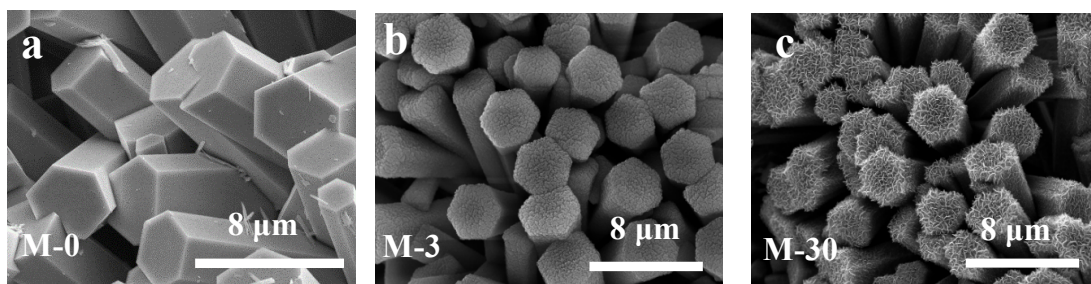


Figure S1. SEM images of M-0, M-3, and M-30

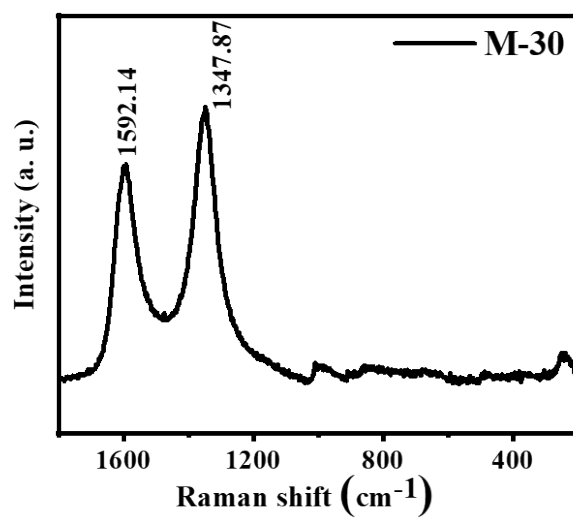


Figure S2. Raman spectra of M-30

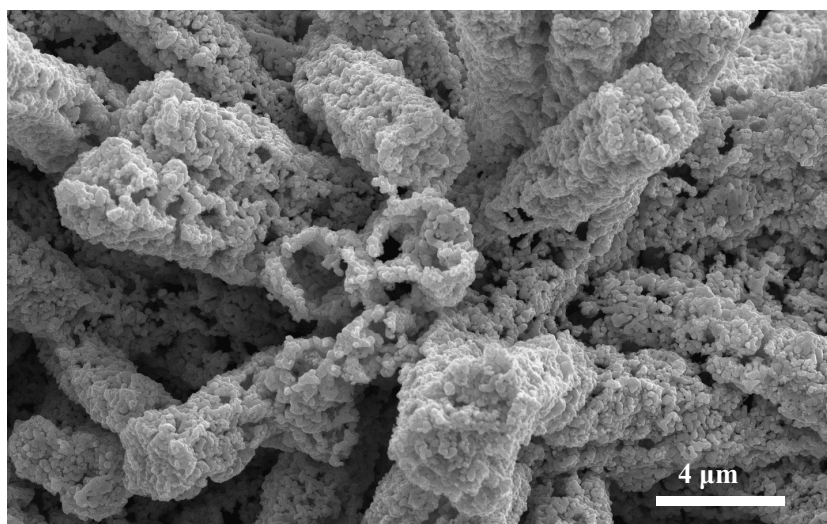


Figure S3. SEM image of M-000

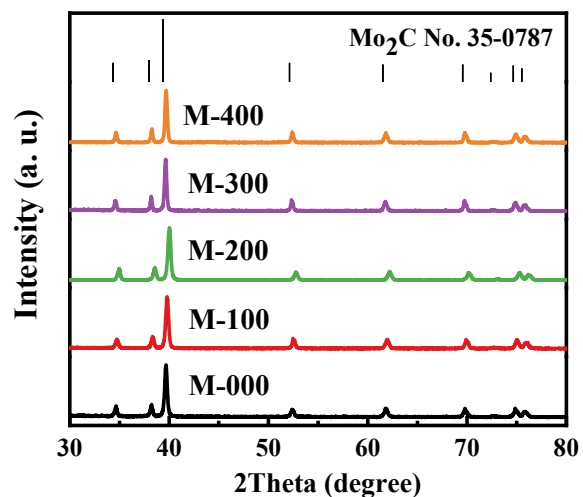


Figure S4. The XRD patterns of M-100, M-200, M-300 and M-400.

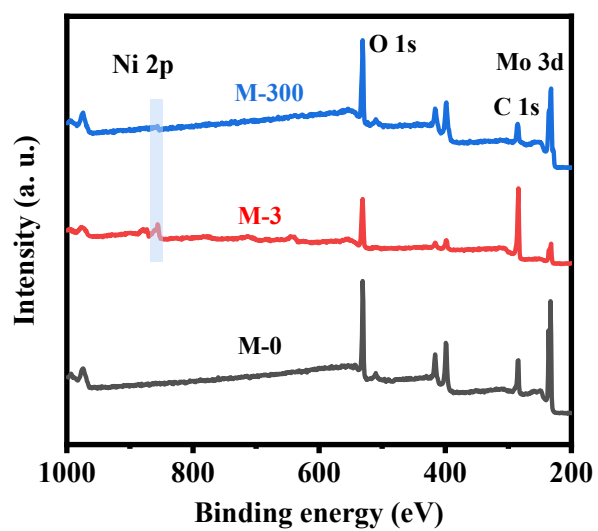


Figure S5. The XPS survey spectra of M-0, M-3, and M-300

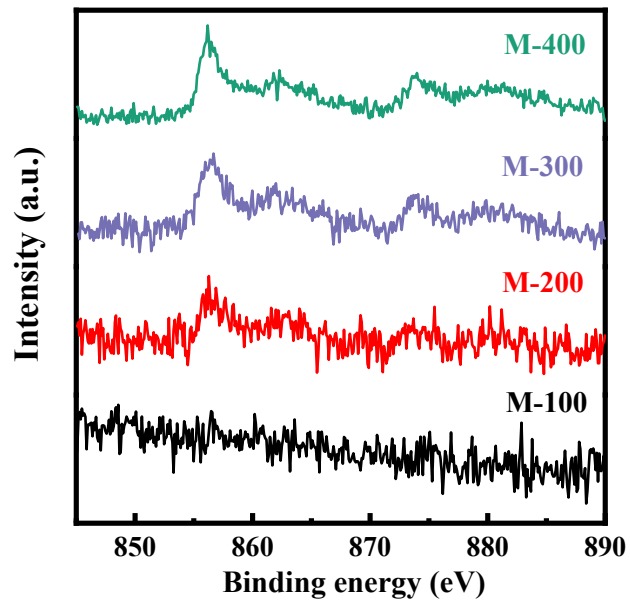


Figure S6. Ni fine spectra of M-100, M-200, M-300 and M-400

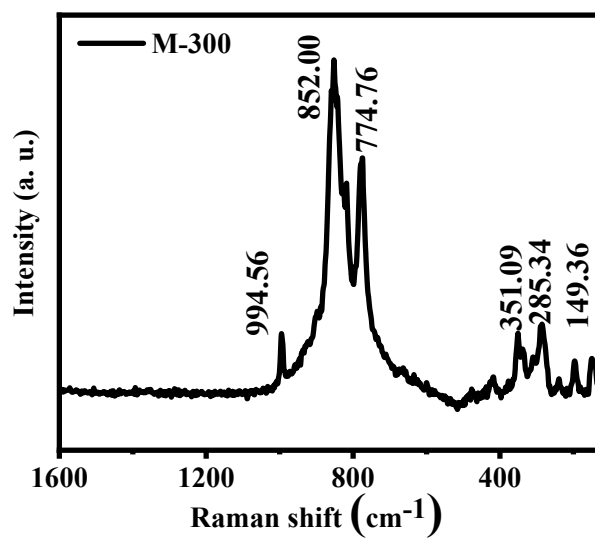


Figure S7. Raman spectrum of M-300

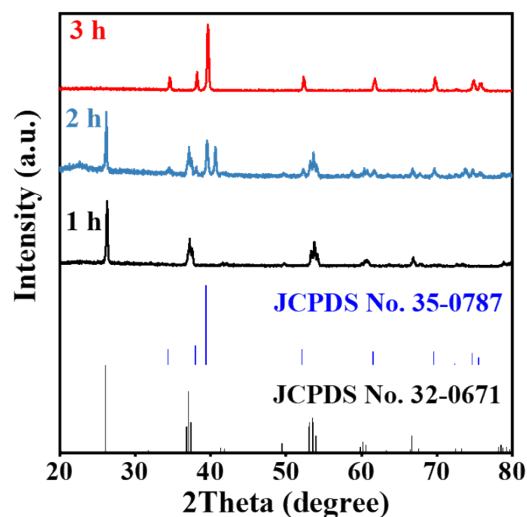


Figure S8. XRD patterns of M-30 calcined at 800°C for different time period.

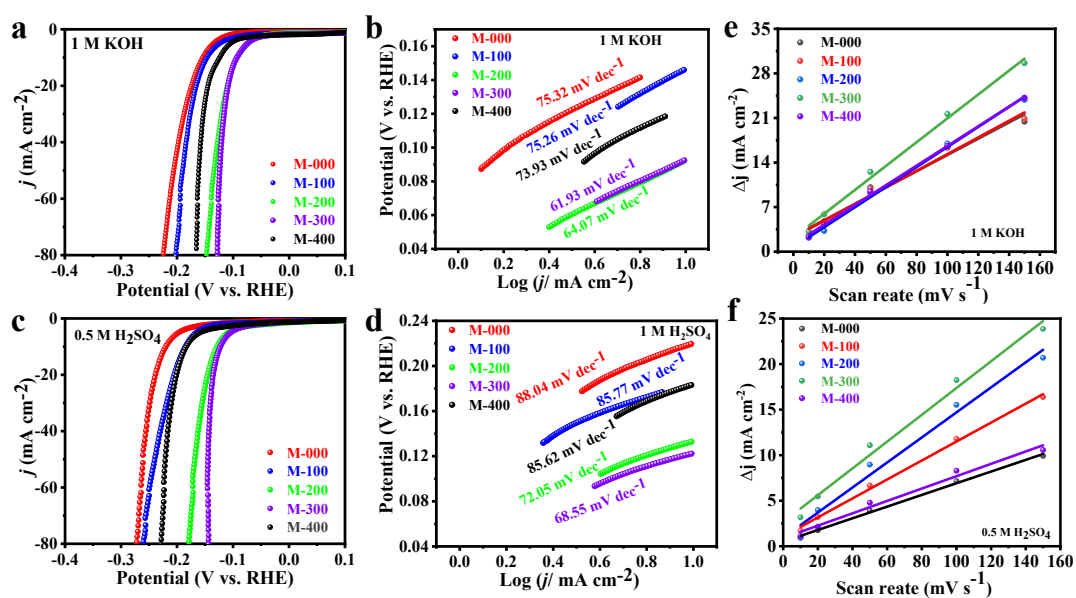


Figure S9. (a) and (c) The LSV curves, (b) and (d) the Tafel plots, (e) and (f) Current density as a function of the scan rate for M-000, M-100, M-200, M-300, and M-400 electrodes.

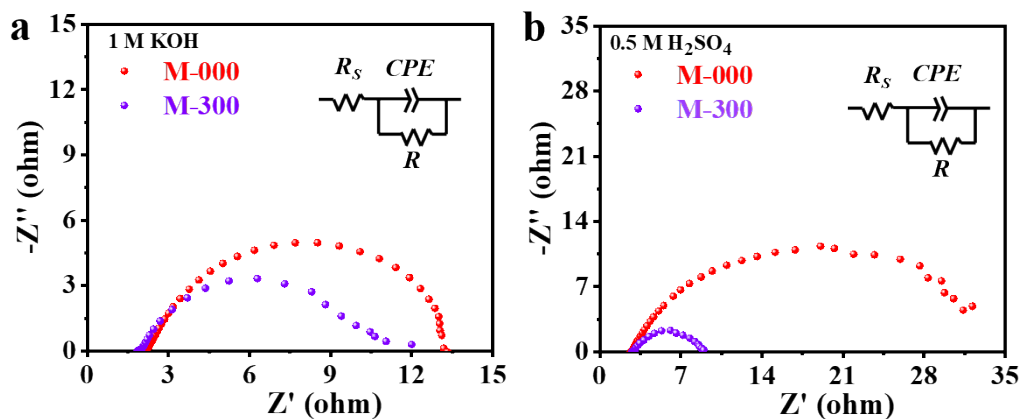


Figure S10. The Nyquist plots of M-000 and M-300.

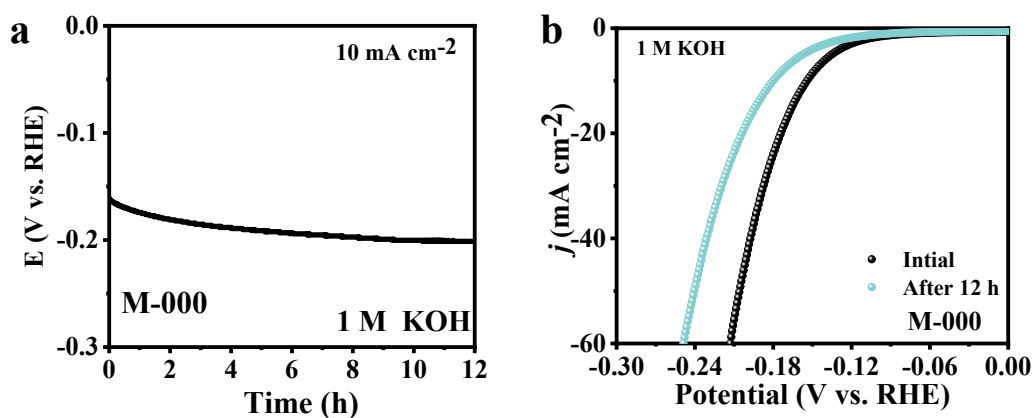


Figure S11. (a) The stability curves (voltage vs. time) and (b) LSV curves of initial and after stability tests in 1 M KOH of the M-000.

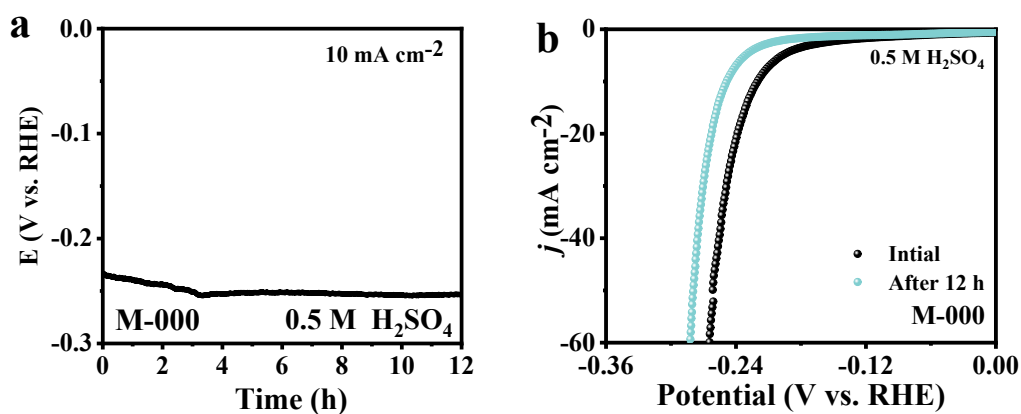


Figure S12. (a) The stability curves (voltage vs. time) and (b) LSV curves of initial and after stability tests in 0.5 M H₂SO₄ of the M-000.

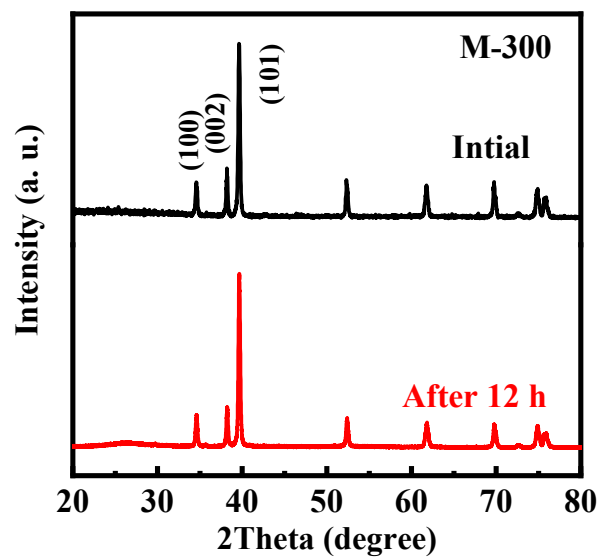


Figure S13. XRD patterns of M-300 before and after stability test in 0.5 M H_2SO_4

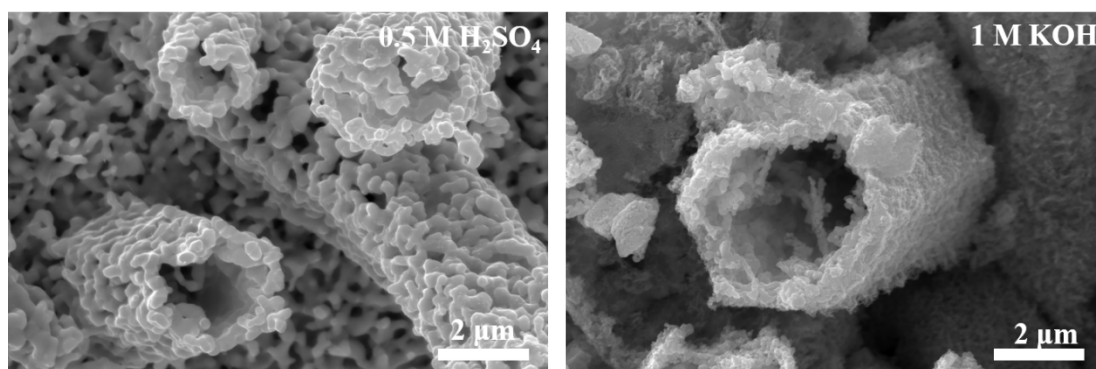


Figure S14. SEM images of M-300 after stability test

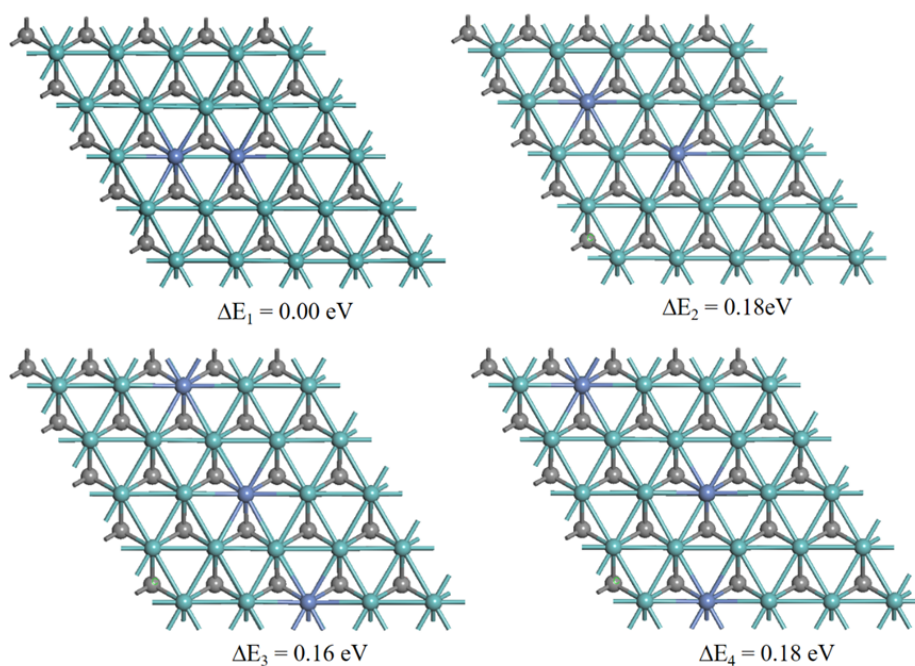


Figure S15. The optimized structures of 2Ni-doped Mo_2C .

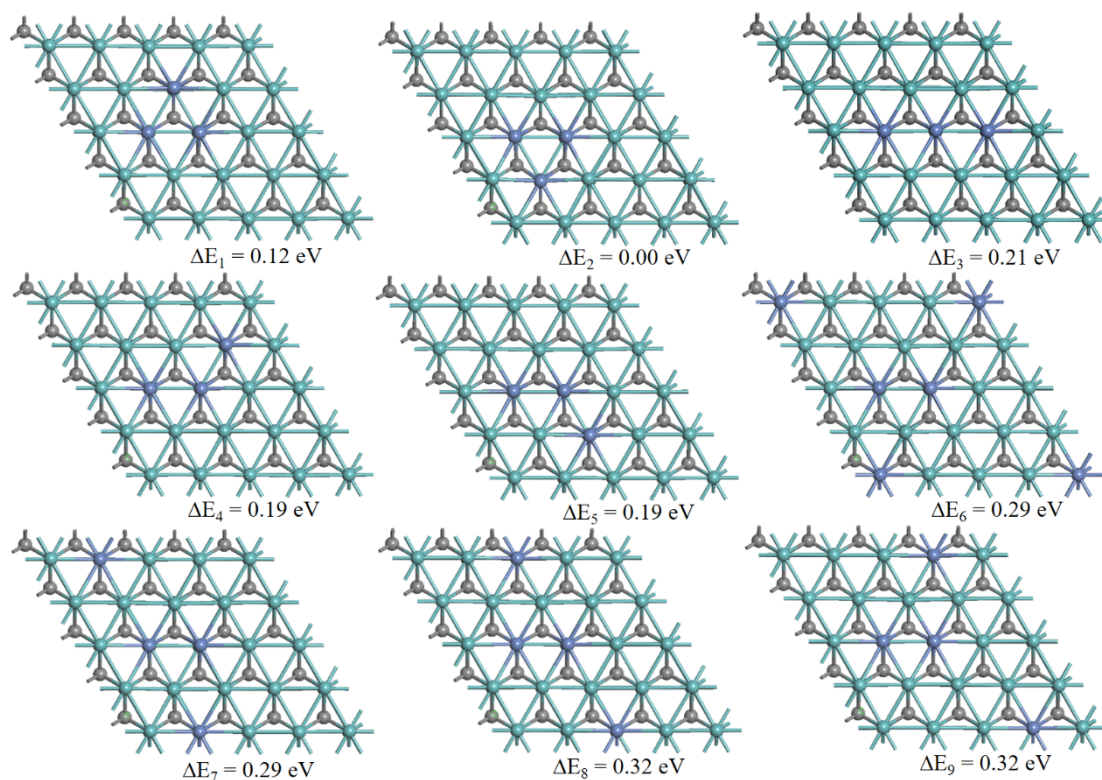


Figure S16. The optimized structures of 3Ni-doped Mo_2C .

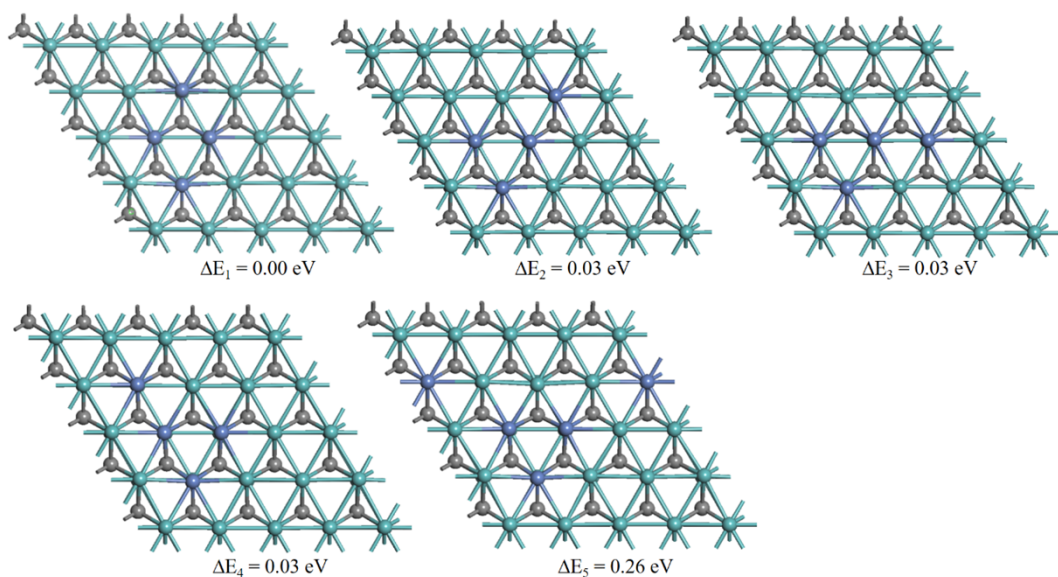


Figure S17. The optimized structures of 4Ni-doped Mo_2C .

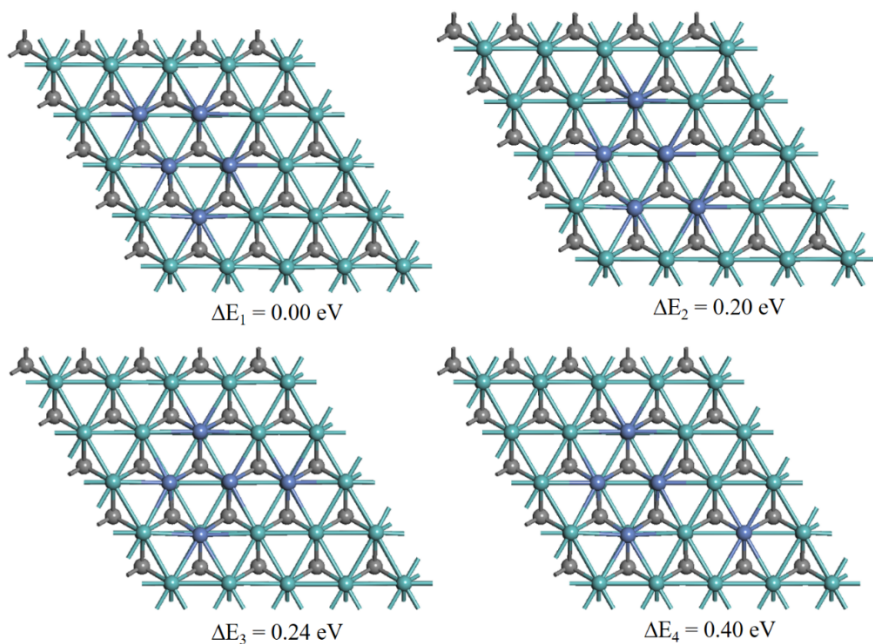


Figure S18. The optimized structures of 5Ni-doped Mo_2C .

Table S1. The content of Ni, Mo, and C was calculated from XPS fine spectra of M-100, M-200, M-300, and M-400.

	M_{Ni} (%)	M_{Mo} (%)	M_{C} (%)
M-100	-	38.00	61.00
M-200	3.53	80.06	16.41
M-300	8.86	75.91	15.22
M-400	10.48	72.08	17.43

Table S2. Comparison of HER electrocatalytic activity of M-300 with other recently reported high performance HER electrocatalysts.

Catalysts	Overpotential (mV) at $j=10 \text{ mA cm}^{-2}$	Electrolyte	Reference
This work (M-300)	93	1 M KOH	
Ni/Mo ₂ C(1:2)-NCNFs	143	1 M KOH	1
Co-NC@Mo ₂ C	99	1 M KOH	2
Co, Mo ₂ C-CNF	128	1 M KOH	3
Co-Mo ₂ C@C	98	1 M KOH	4
Ni/Mo ₂ C-NCSs	131	1 M KOH	5
Co-Mo ₂ C-CN _{x-2}	92	1 M KOH	6
Ni-Mo ₂ C-0.67	151.1	1 M KOH	7
This work (M-300)	122	0.5 M H₂SO₄	
Co-NC@Mo ₂ C	143	0.5 M H ₂ SO ₄	2
Mo ₂ C@NG/CNT	160	0.5 M H ₂ SO ₄	8
Mo ₂ C-GNR	152	0.5 M H ₂ SO ₄	9
Ni-Mo ₂ C-0.67	165	0.5 M H ₂ SO ₄	7
L-Mo ₂ C	170	0.5 M H ₂ SO ₄	10
Mo ₂ C/W ₂ C	140	0.5 M H ₂ SO ₄	11
VN/Mo ₂ C	140	0.5 M H ₂ SO ₄	12

Reference

1. M. Li, Y. Zhu, H. Wang, C. Wang, N. Pinna and X. Lu, *Advanced Energy Materials*, 2019, **9**, 1803185.
2. Q. Liang, H. Jin, Z. Wang, Y. Xiong, S. Yuan, X. Zeng, D. He and S. Mu, *Nano Energy*, 2019, **57**, 746-752.
3. J. Wang, R. Zhu, J. Cheng, Y. Song, M. Mao, F. Chen and Y. Cheng, *Chemical Engineering Journal*, 2020, **397**, 125481.
4. S. Yuan, M. Xia, Z. Liu, K. Wang, L. Xiang, G. Huang, J. Zhang and N. Li, *Chemical Engineering Journal*, 2022, **430**, 132697.
5. Y. Xu, J. Yang, T. Liao, R. Ge, Y. Liu, J. Zhang, Y. Li, M. Zhu, S. Li and W. Li, *Chemical Engineering Journal*, 2022, **431**, 134126.
6. P. Zhang, Y. Liu, T. Liang, E. H. Ang, X. Zhang, F. Ma and Z. Dai, *Applied Catalysis B: Environmental*, 2021, **284**, 119738.
7. W. Liu, X. Wang, J. Qu, X. Liu, Z. Zhang, Y. Guo, H. Yin and D. Wang, *Applied*

- Catalysis B: Environmental*, 2022, **307**, 121201.
8. C. Yang, K. Shen, R. Zhao, H. Xiang, J. Wu, W. Zhong, Q. Zhang, X. Li and N. Yang, *Advanced Functional Materials*, 2021, **32**, 2108167.
 9. X. Fan, Y. Liu, Z. Peng, Z. Zhang, H. Zhou, X. Zhang, B. I. Yakobson, W. A. Goddard, X. Guo, R. H. Hauge and J. M. Tour, *ACS Nano*, 2017, **11**, 384-394.
 10. W. Yuan, Q. Huang, X. Yang, Z. Cui, S. Zhu, Z. Li, S. Du, N. Qiu and Y. Liang, *ACS Applied Materials & Interfaces*, 2018, **10**, 40500-40508.
 11. Y. Ling, F. M. D. Kazim, Q. Zhang, S. Xiao, M. Li and Z. Yang, *International Journal of Hydrogen Energy*, 2021, **46**, 9699-9706.
 12. L. Feng, S. Li, D. He, L. Cao, G. Li, P. Guo and J. Huang, *ACS Sustainable Chemistry & Engineering*, 2021, **9**, 15202-15211.